Metabolite Profiling and Anti-Inflammatory Screening of Ganoderma boninense from Three Malaysian Regions Using LC-MS/MS-Based Molecular Networking

Nur Hidayah Mohd Noor
Department of Chemistry, Faculty of Science, Universiti Putra Malaysia (UPM)

Nadiah Mad Nasir
Department of Chemistry, Faculty of Science, Universiti Putra Malaysia (UPM)

Pavithren Devakrishnan
Department of Chemistry, Faculty of Science, Universiti Putra Malaysia (UPM)

Mohd Rizuan Zainal Abidin
Head of Crop Protection & Bio solutions, FGV Holdings Berhad (HQ)

https://doi.org/10.5109/7395647

出版情報：Proceedings of International Exchange and Innovation Conference on Engineering & Sciences (IEICES). 11, pp.1086-1093, 2025-10-30. International Exchange and Innovation Conference on Engineering & Sciences
バージョン：

Metabolite Profiling and Anti-Inflammatory Screening of *Ganoderma boninense* from Three Malaysian Regions Using LC-MS/MS-Based Molecular Networking

Nur Hidayah Mohd Noor[1], Nadiah Mad Nasir[1], Pavithren Devakrishnan[1], Mohd Rizuan Zainal Abidin[2]
[1]Department of Chemistry, Faculty of Science, Universiti Putra Malaysia (UPM), 43400 UPM Serdang, Selangor, Malaysia,
[2]Head of Crop Protection & Bio solutions, FGV Holdings Berhad (HQ), Wisma FGV, Jalan Raja Laut,50350 Kuala Lumpur, Malaysia.
Corresponding author email: nadiahmadnasir@upm.edu.my

Abstract: Ganoderma boninense *is primarily known as a harmful pathogen responsible for basal stem rot in oil palms, significantly affecting the palm oil industry in Southeast Asia. As a result, farmers often chop down and discard the* G. boninense*. However, recent studies suggest that this discarded material may possess untapped pharmacological potential, including anti-inflammatory properties. The metabolite composition and bioactivity of* G. boninense *are influenced by environmental factors, which can limit its consistency. In this study, advanced techniques such as LC-MS/MS and molecular networking (MN) were used to annotate groups of triterpenoids, alkaloids, and aminoglycosides from samples collected at three different locations in Malaysia. All crude extracts were evaluated for their inhibitory effects on LPS-induced nitric oxide (NO) production in murine macrophage RAW264.7 cells. All three* G. boninense *extracts significantly suppressed NO production, with effective concentrations ranging from 0.50 to 0.60 µM which comparable to the effect of the positive control, dexamethasone.*

Keywords: Molecular Networking; Ganoderma; LC-MS/MS; Cytotoxic; Anti-inflammatory

1. INTRODUCTION

The Ganoderma genus, belonging to the Ganodermataceae family, is globally recognized for its notable medicinal properties. However, many Ganoderma species are also known to cause white rot in hardwoods by breaking down lignin, cellulose, and related polysaccharides [1]. They are typically associated with the decay of roots and the lower trunk or stem flare, which can lead to structural instability in trees, posing serious risks to property and human safety [1]. Globally, there are 131 identified Ganoderma species, with around 20 species, including *Ganoderma lucidum, Ganoderma lingzhi,* and *Ganoderma sinense* proven through modern research to possess medicinal value. Ganoderma species are predominantly found in tropical and subtropical regions across Africa, the Americas, Asia, and Oceania [2].

Among the many species, *G. lucidum* stands out due to its long-standing use in traditional medicine and extensive scientific research. Commonly known as Reishi or Lingzhi in Chinese medicine, *G. lucidum* is recognized as a premium herbal remedy [3]. It has been traditionally used to treat various health conditions, including chronic hepatitis, hypertension, and bronchitis. Its notable therapeutic properties have earned it a reputation as a powerful immune system booster. The species contains over 400 bioactive compounds, such as triterpenoids, polysaccharides, nucleotides, sterols, steroids, fatty acids, and peptides [4]. Studies have consistently highlighted its pharmacological potential, including anti-tumor [5], antibacterial [6], anti-inflammatory [7], and antiviral [8] effects. Referred to as the "superior herb" or "mushroom of immortality" [4], *G. lucidum* is known for its health-promoting effects and safe, long-term use without side effects.

Conversely, a closely related species, *Ganoderma boninense*, is best known not for medicinal use but as a destructive fungal pathogen affecting oil palm trees in Southeast Asia [9]. It is the primary cause of basal stem rot disease, which can infect oil palms at any growth stage, significantly reducing palm oil yields [10-11]. Despite its role as a major pathogen, limited research has been devoted to exploring its potential bioactive compounds. However, recent findings suggest that *G. boninense* may possess pharmacological properties comparable to those of *G. lucidum*. Li *et al*., [10] have reported that polysaccharides extracted from *G. boninense* have shown promising antioxidant activity.

These emerging findings highlight the dual nature of *G. boninense*, both as a harmful pathogen and a source of valuable medicinal compounds. Importantly, research has shown that geographic variation may influence the metabolite profiles of fungi within the same species. Factors such as soil composition, temperature, humidity, and microbial interactions are believed to play a role in these differences [12]. To date, no comparative study has systematically examined how these environmental factors affect the presence of bioactive compounds in *G. boninense*. Understanding this relationship could be key to identifying specific regions where the species has greater therapeutic potential.

Liquid chromatography coupled with tandem mass spectrometry (LC-MS/MS) is a powerful and advanced analytical tool widely used for profiling bioactive compounds [13]. According to Shankar and Sharma [14], this technique offers high-resolution detection of structurally diverse compounds in complex biological extracts. Together with LC-MS/MS, it is effective for metabolite identification; the integration of molecular networking (MN) enhances its capabilities by clustering

data based on molecular structures. MN allows for the visualization of structural relationships among compounds within the same molecular family, thereby simplifying the identification of unknown metabolites [15].

A report by Dai et al., [16] utilized Activity Labeled Molecular Networking (ALMN) to screen metabolites from *Dendrobium officinale*, successfully identifying five compounds with anti-inflammatory properties. Similarly, Marques et al. [17] discovered anti-tumor compounds in Withania species through the combined use of LC-MS/MS and the Global Natural Products Social Molecular Networking (GNPS) platform. Applying these techniques to *G. boninense* could allow for the visualization of structurally related compounds and the potential discovery of novel metabolites. However, there remains a notable gap in current studies, as such integrated approaches have yet to be applied to the study of *G. boninense*.

Inflammation contributes to the development of numerous chronic diseases, including cancer, diabetes, arthritis, and cardiovascular disorders [18]. This highlights the importance of discovering effective anti-inflammatory agents, particularly from natural sources. In recent years, fungi and medicinal plants have played a vital role in the discovery of novel anti-inflammatory compounds [19].
For instance, *Chlorella vulgaris* extracts have shown anti-inflammatory activity, acting by inhibiting the production of nitric oxide (NO), tumor necrosis factor-alpha (TNF-α), and interleukin-6 (IL-6) [20]. In this context, screening *G. boninense* for anti-inflammatory metabolites, combined with LC-MS/MS-based molecular networking, enhances compound identification and deepens understanding of its therapeutic potential.

Despite growing evidence highlighting the significant pharmacological potential of *G. boninense,* the species remains largely underexplored, particularly in the context of advanced analytical techniques such as LC-MS/MS combined with molecular networking. Additionally, variations in bioactivity among *G. boninense* samples from different geographical locations have not yet been systematically investigated. These gaps in current knowledge form the basis of this study.

This research aims to profile and annotate metabolites extracted from *G. boninense* obtained from FGV Holdings Berhad, collected from three distinct geographic regions of Malaysia, which are Serting (Negeri Sembilan), Ulu Belitong (Kluang) and Jengka (Pahang) using LC-MS/MS-based molecular networking. Concurrently, the study will evaluate the anti-inflammatory activity of these extracts to identify candidate compounds with therapeutic relevance. This work is expected to contribute valuable insights into the bioactive metabolite profile of *G. boninense*, supporting future drug discovery efforts and promoting the development of natural product-based therapeutics.

2. MATERIALS AND METHODS

2.1 Sample Collection

The three samples of *G. boninense* were obtained from FGV Holdings Berhad (HQ), Wisma FGV, Jalan Raja Laut, 50350 Kuala Lumpur, Malaysia. They were collected from their oil palm plantations, which are located in Serting (Negeri Sembilan), Ulu Belitong (Kluang) and Jengka (Pahang). The different locations are to account for possible metabolite variations across geographical and environmental factors. The samples are kept in a biohazard bag until further analysis at 4ºC.

2.2 Extraction of *G. boninense* Fruiting Bodies

The fruiting bodies from all three *G. boninense* samples were washed, gently dried with a paper towel, and cut into smaller pieces. They were then stored at −80 °C for three days before undergoing freeze-drying. Once freeze-dried, the samples were ground into a fine powder using a mechanical grinder. As shown in Fig.1, the fresh samples were collected from three different geographic locations. For the extraction process, a solid-to-solvent ratio of 1:25 was applied, as this ratio has been reported to yield a high concentration of triterpenes [21]. Specifically, 100 g of each powdered sample was soaked separately in 2500 mL of ethyl acetate for two weeks under low-light conditions. Ethyl acetate was selected for its moderate polarity, making it suitable for extracting a broad range of metabolites, including triterpenes and polysaccharides. Moreover, a study by Chan and Chong [22] demonstrated that ethyl acetate yielded the highest concentration of metabolites among the solvents tested.
After the two-week extraction period, the mixtures were filtered and concentrated using a rotary evaporator at 45 °C to obtain crude extracts. The remaining traces of ethyl acetate were removed by placing the extracts under a fume hood for three days. Finally, the dried crude extracts were weighed and stored at −20 °C in preparation for LC-MS/MS analysis (Fig. 2).

Fig. 1. The fresh sample of *G. boninense* from three different locations.

Fig. 2. The crude extracts with their masses.

2.3 LC-MS/MS Analysis

The LC-MS/MS analysis of crudes was performed according to [16; 23]. Each crude extract was reconstituted in LC-MS grade methanol at a concentration of 2 mg/mL and filtered through a 0.22 µm syringe filter before analysis. LC-MS/MS analysis was performed using an ultra-high-performance liquid chromatography (UHPLC) system coupled with a high-resolution Orbitrap mass spectrometer and an electrospray ionization (ESI) source at the Institute of Bioscience (IBS), Universiti Putra Malaysia. Liquid chromatography was conducted on a Thermo Scientific Dionex Ultimate 3000 UHPLC system equipped with a Hypersil GOLD Aq reverse-phase column (100 × 2.1 mm, 1.9 µm particle size), maintained at 40 °C throughout the analysis.

The mobile phase consisted of solvent A (water with 0.1% formic acid) and solvent B (acetonitrile with 0.1% formic acid). Gradient elution was programmed as follows: starting at 2% B, maintained until 0.5 minutes, then gradually increased to 50% at 18 minutes. This was followed by an increase to 98% B at 24 minutes, held up to 26 minutes. The system was then returned to the initial condition (2% B) at 28 minutes and maintained for 2 minutes to re-equilibrate the column, resulting in a total run time of 30 minutes. The flow rate was set at 0.4 mL/min, with an injection volume of 5 µL.

Mass spectrometry data were acquired using a Thermo Scientific Q Exactive Focus Orbitrap mass spectrometer with a heated electrospray ionization (HESI) source, operated in both positive and negative ionization modes in separate runs. Data acquisition was carried out in polarity switching mode, using a data-dependent MS^2 (dd-MS^2) workflow for compound discovery.

2.4 Data Processing and Molecular Networking

The raw LC-MS/MS data were converted to the mzML format using MSConvert (ProteoWizard), with the negative ionization mode selected exclusively. The mzML files were then processed using MZmine version 4.5.0 to extract MS/MS spectral information. For molecular networking, the processed mzML files were uploaded to the Global Natural Products Social Molecular Networking (GNPS) platform via the FileZilla FTP client. Once the upload was complete, the data were analyzed through the GNPS web platform (https://gnps.ucsd.edu, accessed on 7th February 2025). Detailed metabolite data from the crude extracts can be accessed at the following GNPS workflow link: http://gnps.ucsd.edu/ProteoSAFe/status.jsp?task=55777e5d95a64583b4b357f098c47001 (accessed on 25th February 2025). Upon completion of the workflow, the resulting molecular network files were exported in GraphML format and visualized using Cytoscape software (version 3.10.3). A force-directed layout was applied to facilitate structural clustering and compound annotation [16].

2.5 Anti-Inflammatory Activity Assay

The assessment of anti-inflammatory activity was conducted by an external research laboratory at the Malaysian Nuclear Agency. The study adhered to established methodologies as described in previous literature [24-25]. Specifically, the RAW 264.7 murine macrophage cell line was employed to evaluate the anti-inflammatory potential of three crude extracts derived from *G. boninense*. The evaluation included the MTT assay to determine cell viability and the Griess assay to measure nitric oxide (NO) inhibition.

2.5.1 Cell Culture

The RAW 264.7 murine macrophage cells were obtained from a reputable cell repository. They were cultured in Dulbecco's Modified Eagle's Medium (DMEM) supplemented with 10% fetal bovine serum (FBS) and 1% penicillin-streptomycin. The culture temperature was maintained at 37°C with 5% CO_2 to ensure a humidified and optimal environment.

2.5.2 Extract Preparation

The crude extracts of *G. boninense* were dissolved in dimethyl sulfoxide (DMSO), ensuring that the final concentration of DMSO did not exceed 0.1% to minimize solvent-induced cytotoxicity. The extracts were then sterilized by filtration through 0.22 µm membrane filters and subsequently prepared in a series of concentrations (0, 1.95, 3.91, 7.81, 15.63, 31.25, 62.50, 125.00, 250.00, 500.00, 1000.00, and 2000.00 µg/mL) for use in treatment assays.

2.5.3 Cell Viability Assay (MTT)

To assess cytotoxicity and establish a safe concentration range, an MTT assay was conducted following the method described by Senghoi et al. [24]. RAW 264.7 cells were seeded in 96-well plates at a density of 1×10^4 cells per well and incubated overnight to allow cell adherence. Subsequently, the cells were treated with varying concentrations of *G. boninense* extract for 96 hours. Following treatment, 20 µL of MTT solution (5 mg/mL) was added to each well, and the plates were incubated for an additional 4 hours. The resulting formazan crystals were solubilized using DMSO, and absorbance was measured at 570 nm using a spectrophotometer. All experiments were performed in quadruplicate to ensure accuracy and reproducibility. The IC_{50} values were determined by comparing treated samples to the negative control. The concentration of extract required to induce 50% cytotoxicity in RAW 264.7 cells was derived from a dose-response curve plotting cell viability against extract concentration. The percentage of cell viability was calculated using the following equation:

$$\text{Cell viability (\%)} = \left(\frac{\text{Absorbance of sample}}{\text{Absorbance of control}}\right) \times 100$$

2.5.4 Nitric oxide (NO) level measurement

To evaluate the inhibition of nitric oxide (NO) production, the Griess assay was performed. RAW 264.7 cells were seeded in 96-well plates and pre-treated with varying concentrations of the extract for 1 hour before stimulation with 1 µg/mL of lipopolysaccharide (LPS). The assay protocol was adapted from the study by Senghoi et al. [24]. Following a 24-hour incubation period, 100 µL of the culture supernatant was collected from each well and mixed with an equal volume of Griess reagent (sulfanilamide and *N*-(1-naphthyl) ethylenediamine dihydrochloride). Absorbance was measured at 570 nm using a spectrophotometer, and nitric oxide levels were quantified based on a standard curve generated with known concentrations of NO.

3. RESULTS AND DISCUSSION

3.1 Metabolites Profiling from LC-MS/MS analysis of Three Different Locations

The metabolites in the *G. boninense* extracts were analyzed using LC-MS/MS, and the resulting mass fragmentation patterns were matched against a spectral database of previously identified compounds. A combined total ion chromatogram (TIC) from various locations (Serting, Ulu Belitong, Jengka) was generated for comparative analysis, as shown in Fig. 3. Only peaks with significant intensity were selected for annotation, reflecting the high concentration and potential biological relevance of the metabolites. To ensure consistency, the minimum base peak intensity was set at 5.0×10^7 across all chromatographic data, resulting in the identification of 15 metabolites.

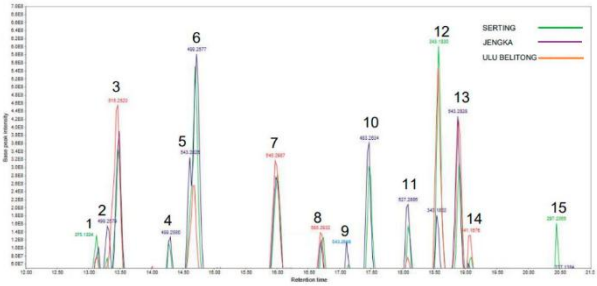

Fig. 3. The total ion chromatograms (TIC) for each of the sample based on locations, (---) Serting, (---) Jengka and (---) Ulu Belitong.

As shown in Fig. 3, the different colors of each peak correspond to their respective sample locations, indicating the presence of metabolites in various samples. Some peaks display only certain colors, initially suggesting the absence of those metabolites in other locations. However, further analysis using MZmine 4.5.0 revealed that the metabolites were indeed present in those locations but expressed at below the 5.0×10^7 of base peak intensity. Compound annotation was carried out by comparing the m/z values of the detected peaks with those of previously identified compounds [4, 8, 22, 26-33]. The mass fragmentation patterns provided spectral matches, enabling the putative identification of the metabolites. It is observed from the TIC of all three crudes that the peaks of 3, 6, 7, 10, 12 and 13 are among the major metabolites extracted. These compounds are annotated as in Table 1. The major metabolites belong to groups of triterpenoids, alkaloids and amino glycosides.

Interestingly, we annotated that peak 6 is Ganolucidic acid A, appeared as major in Serting and Jengka crudes, while minor in the Ulu Belitong crude. Another major peak, at peak 12**,** is annotated as (Methyl (2R,3R,4S)-3-acetamido-4-(diaminomethylideneamino)-2-(propylcarbamoyl)-3,4-dihydro-2H-pyran-6-carboxylate has appeared as a major metabolite in the Serting and Ulu Belitong crudes and minor in the Jengka. This is because location can lead to factors that shape the plant's environment, which directly or indirectly influences its biochemical pathways, leading to variations in metabolite composition, concentration, and diversity. This is why plants or fungi of the same species collected from different regions can show different metabolite profiles.

Table 1. Annotated compounds based on LC-MS/MS and MN in all samples of *G. boninense.*

Peak	$[M-H]^-$ (m/z)	MS/MS (m/z)	Proposed Compound	References
1	275	275, 245, 231	6-ethoxy-2-(2-phenylethenyl)quinoline	Chan & Chong, (2020); Singh et al. (2014)
2	499	499, 481, 455	Ambruticin VS3	Chan & Chong, (2020); Vetcher et al. (2007)
3	515	515, 497, 471, 443	Ganoderic acid B	Katarzyna Sulkowska-Ziaja et al. (2023); Sanodiya et al., 2009
4	499	499, 455, 359	Ganoderic acid GS-2	Sato et al. (2009)
5	543	543, 499, 427	N-epsilon-(Octanoyl)lysyl-uracil polyoxin C	Chan & Chong, (2020)
6	499	499, 481, 455, 427, 409, 397, 355	Ganolucidic acid A	Sanodiya et al. (2009); Castellano and Torrens (2015); Sanodiya et al., 2009
7	545	545, 499, 485, 409, 327	Unknown	-
8	585	585, 567, 549	Amikacin	Chan & Chong, (2020);
9	543	543, 413, 399	Americine	Chan & Chong, (2020)
10	483	483, 371	12α-methoxy-ganodermanondiol	Chen et al. (2023)
11	527	527, 483, 467	(2*R*,3*S*,4*R*,5*R*,6*R*)-2-(aminomethyl)-5-(3-aminopropylamino)-6-[(2*S*,3*S*,4*R*,6*S*)-4,6-diamino-3-[(2*S*,3*R*,5*S*,6*R*)-3,5-dihydroxy-6-(hydroxymethyl)oxa	PubChem (assessed on 11th May 2025)

			n-2-yl]oxy-2-hydroxycyclohexyl] oxyoxane-3,4-diol	
12	343	343, 300, 298, 285	Methyl (2*R*,3*R*,4*S*)-3-acetamido-4-(diaminomethylideneamino)-2-(propylcarbamoyl)-3,4-dihydro-2H-pyran-6-carboxylate	PubChem (assessed on 11th May 2025)
13	543	543, 483, 411	N-[(1*S*,2*R*,3*R*,4*S*,5*R*,6*R*)-5-amino-2-[(2*S*,3*R*,4*R*,5*S*,6*R*)-3-amino-4,5-dihydroxy-6-(hydroxymethyl)oxan-2-yl]oxy-4-[(2*S*,3*R*,4*S*,5*S*,6*R*)-4-amino-3,5-dihydroxy-6-(hydroxymethyl)oxan-2-yl]oxy-3,6-dihydroxycyclohexyl]acetamide	PubChem (assessed on 11th May 2025)
14	341	341, 297, 279, 159	4-Acetyl-4-guanidino-6-methyl(propyl) carboxamide-4,5-dihydro-2H-pyran-2-carboxylic acid	Chan & Chong, (2020); Srinivas et al. (2014)
15	297	297, 279, 183	(2*R*,3*R*,4*S*)-3-acetamido-4-guanidino-2-(methylcarbamoyl)-3,4-dihydro-2H-pyran-6-carboxylic acid	PubChem (assessed on 11th May 2025)

3.2 LC-MS/MS-based Molecular Networking Analysis

The LC-MS/MS data were further analyzed through GNPS-based molecular networking, enabling the visualization of metabolite clusters. Fig. 4 illustrates the metabolite clusters identified in *G. boninense* across the samples. Overall, three major distinct clusters and four groups of single nodes were observed. Each of the major clusters exhibited similar fragmentation patterns.

The molecular network (MN) analysis revealed three major metabolite clusters obtained in all the crudes (Fig. 4), corresponding to alkaloids, triterpenoids, and aminoglycosides. Within the triterpenoid cluster, three compounds were identified and showed the same backbone structure: ganoderic acid B (**3**), ganoderic acid GS-2 (**4**), and ganolucidic acid A (**6**). Among them, ganoderic acid B (**3**) and ganolucidic acid A (**6**) were the predominant triterpenoids detected across all crudes, as confirmed by LC-MS/MS data (Fig. 3).

Ganoderic acid B (**3**) was detected with a precursor ion at m/z 515 $[M–H]^-$ and a retention time (RT) of 13.46 minutes (peak 3). It exhibited a fragment ion at m/z 359, corresponding to the loss of 2,6-dimethyl-4-oxoheptanoic acid. Ganolucidic acid A (**6**), with a precursor ion at m/z 499 $[M–H]^-$ and RT of 14.7 minutes (peak 6), displayed a fragmentation pattern matching entries in the spectral database. The presence of a fragment ion at m/z 427 is consistent with previous reports in *G. lucidum* [29]. Both compounds demonstrated mass spectral similarity to known fragmentation patterns and matched confidently with reference spectra.

The next major cluster found in the resulting network is the alkaloids, which comprise quinoline and guanidine alkaloids. Three guanidine alkaloids showed almost identical structures and were observed at peaks 12, 14, and 15. Interestingly, peak 12 was identified as methyl

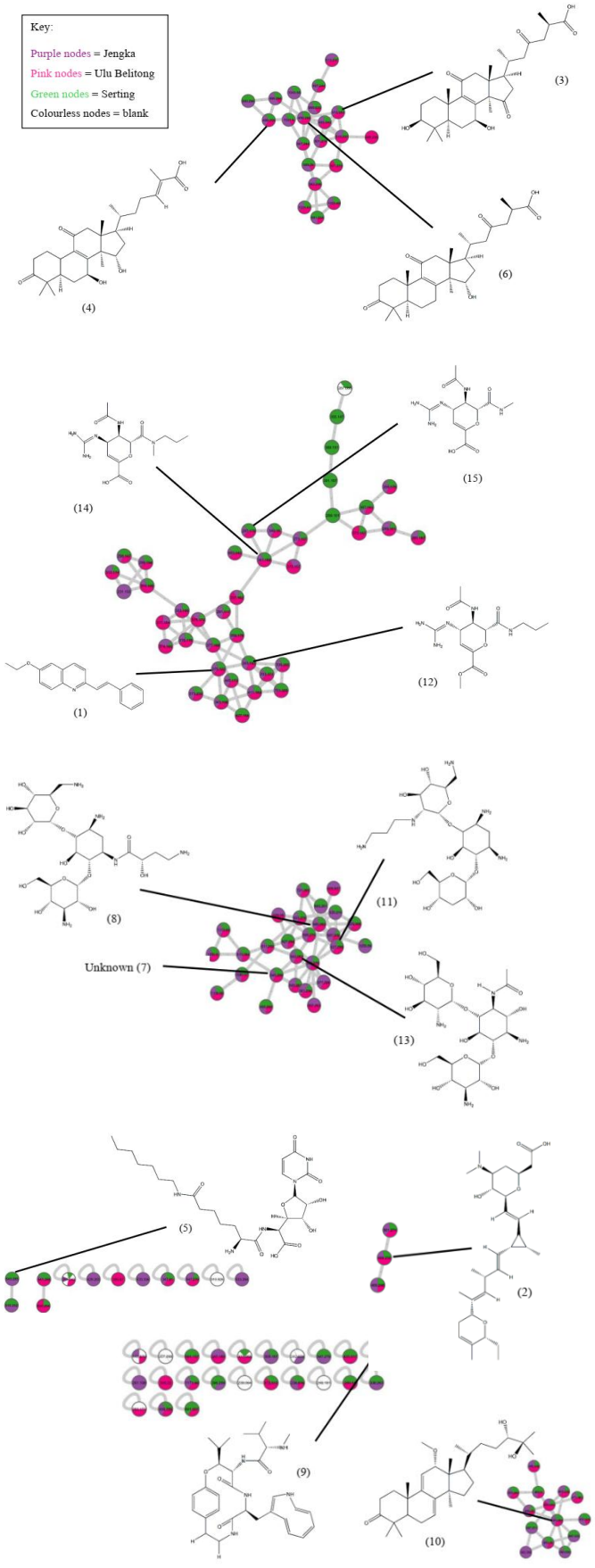

Fig. 4. Annotation of the molecular networking of the metabolites in all samples of *G. boninense,* obtained from the GNPS library and PubChem platforms.

(2*R*,3*R*,4*S*)-3-acetamido-4-(diaminomethylideneamino)-2-(propylcarbamoyl)-3,4-dihydro-2H-pyran-6-carboxylate, with a precursor ion of m/z 343 [M]+ and a retention time (RT) of 18.56 minutes. It appeared as the most abundant compound in the Serting and Ulu Belitong crude extracts but was less abundant in the Jengka crude (Fig. 3). This compound (peak 12) matched the MS/MS fragmentation pattern and was aligned with data from [32]. The quinoline alkaloid, identified as 6-ethoxy-2-(2-phenylethenyl), had a precursor ion of m/z 275 [M]+ and a retention time of 13.12 minutes (peak 1). It was detected with fragment ions at m/z 245 and m/z 231. This compound also matched the MS/MS fragmentation pattern and was consistent with findings reported by Chan and Chong [22].

The third major cluster identified in the molecular networking analysis corresponds to the aminoglycoside class. Although four metabolites were annotated within this cluster, only three could be confidently matched to reference spectra [22];[32]. These three compounds exhibit a similar structural motif, characterized by three rings connected via oxygen linkages. The identified metabolites are detailed in Table 1. Amikacin was identified at m/z 585 [M] with a retention time of 16.7 minutes (peak 8), and its identity was supported by characteristic fragment ions at m/z 567 and m/z 549. The other two compounds were detected at m/z 527 $[M+2H]^+$ (peak 11) and m/z 543 $[M+H]^+$ (peak 13), respectively. Unfortunately, we were unable to annotate the compound at peak 7 with m/z 545. However, with the aid of molecular networking clustering, we were able to predict the backbone structure of the unknown compound. Further work is required, including isolation of the compound and its characterization using spectroscopic techniques.

3.3 Anti-Inflammatory Activity of Crude Extracts

In this study, an MTT assay was conducted to determine the appropriate concentrations of all samples for subsequent nitric oxide (NO) inhibition assays using the lipopolysaccharide (LPS)-induced RAW 264.7 cell model. The assay evaluated the effects of the positive control drug dexamethasone, and varying concentrations (1.95–2000 µg/mL) of the extract samples on cell viability. Cell viability percentages were calculated by comparing the absorbance values of treated samples with those of untreated control. Based on these results, half-maximal inhibitory concentration (IC_{50}) values were calculated and are presented in Table 2.

The findings revealed that the extract samples exhibited low cytotoxicity toward RAW 264.7 cells, maintaining cell viability above 50%, with the maximum safe concentration ranging from 82 to 86 µg/mL. Specifically, the Jengka extract demonstrated an IC_{50} value of 85.54 ± 1.33 µg/mL, while the Serting and Ulu Belitong extracts showed slightly lower IC_{50} values of 82.53 ± 0.88 µg/mL and 82.19 ± 0.09 µg/mL, respectively (Table 2). Although the differences among the crude extracts were minimal, the results indicate that *G. boninense* exerts only mild cytotoxic effects (Fig. 5). According to the National Cancer Institute (NCI), a crude extract is considered cytotoxic if it has an IC_{50} value below 20 µg/mL [34]. Thus, our extracts, with IC_{50} values well above this threshold, can be considered to have low cytotoxicity and supporting their potential for the identification of therapeutic compounds with minimal toxicity.

Table 2. The IC_{50} values for RAW 264.7 cells treated with all sample of *G. boninense*.

Extract	IC_{50} (µg/mL)
Jengka	85.54 ± 1.33
Serting	82.53 ± 0.88
Ulu belitong	82.19 ± 0.09

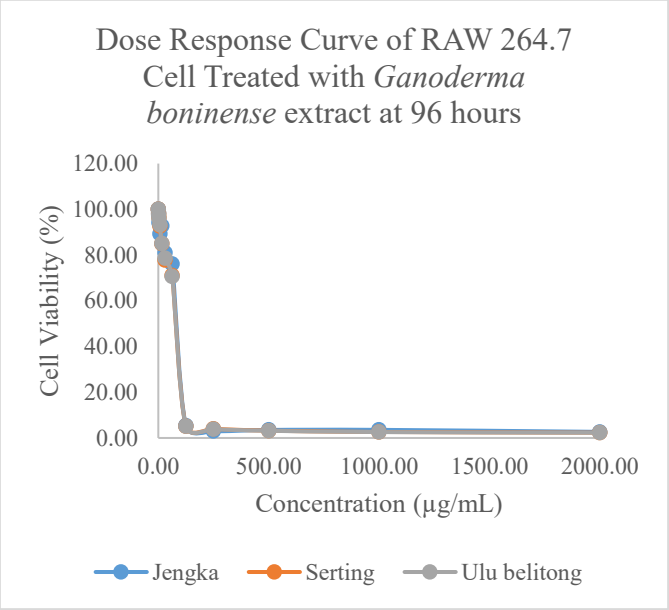

Fig. 5. Dose response curve of RAW 264.7 cells treated with all sample of *G. boninense*.

To evaluate the effect of *G. boninense* extracts on nitric oxide (NO) production in RAW 264.7 cells, the cells were first stimulated with lipopolysaccharide (LPS, 1 µg/mL) for 1 hour. Absorbance was measured at 570 nm, and NO concentrations were calculated using a standard curve. A calibration curve was constructed using sodium nitrite standards (0–100 µM), and nitrite levels in the culture supernatants were quantified for all control and extract-treated samples.

Linear regression of the mean absorbance values at 570 nm produced an R^2 value of 1.0 (Fig. 6), indicating excellent linearity of the standard curve. LPS stimulation alone resulted in the production of 17.44 µM of NO, whereas treatment with dexamethasone reduced NO levels to 0.50 µM, thereby validating the assay. All three *G. boninense* extracts significantly suppressed NO production, with concentrations ranging from 0.50 to 0.60 µM, which closely matched with the effect of the

positive control, dexamethasone (Fig. 7). Although there were slight variations among the extracts, all demonstrated comparable inhibition to dexamethasone, highlighting their strong in vitro anti-inflammatory potential.

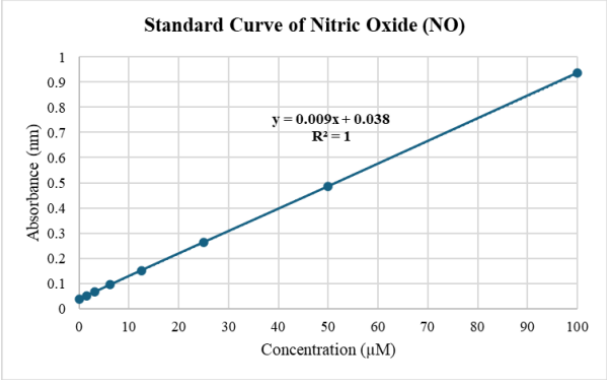

Fig. 6. Standard curve of nitric oxide (NO) showing an R2 value of 1

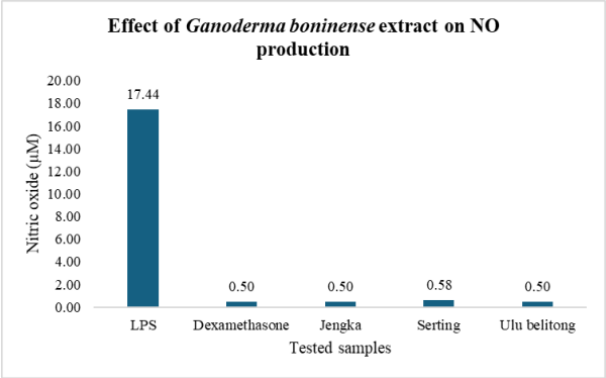

Fig. 7. The effects of *G. boninense* extracts on NO production

4. CONCLUSION

The present study highlights the phytochemical profile of *G. boninense* collected from three regions in Malaysia: Serting (Negeri Sembilan), Ulu Belitong (Kluang), and Jengka (Pahang). Using LC-MS/MS analysis, a total of 15 metabolites were annotated. The observed anti-inflammatory activities of the extracts may be attributed to their high content of triterpenoids, alkaloids, and aminoglycosides, particularly due to the predominant presence of Ganolucidic acid A (**6**) and Methyl (2R,3R,4S)-3-acetamido-4- (diaminomethylideneamino)-2-(propylcarbamoyl)-3,4-dihydro-2H-pyran-6-carboxylate (**12**), as identified through LC-MS/MS. This study provides foundational data supporting the potential of *G. boninense* as an anti-inflammatory agent and point out the need for further *in vivo* investigations and other bioactivities assay [35] to validate its biological activity.

5. REFERENCES

[1]. J. He, X. Han, Z-L. Luo, E-X. Li, S-M. Tang, H-M. Luo, K-Y. Niu, X-J. Su, S-H. Li, Species diversity of Ganoderma (Ganodermataceae, Polyporales) with three new species and a key to Ganoderma in Yunnan Province, China. Front. Microbiol. 13 (2022) 1035434.

[2]. L. Wang, J-Q. Li, J. Zhang, Z-M. Li, H-G Liu, Y-Z. Wang, Traditional uses, chemical components and pharmacological activities of the genus Ganoderma P. Karst.: a review. RSC Adv. 10 (2020) 42084–42097.

[3]. K. M. A. Daruliza, L. Fernandez, R. Jegathambigai, S. Sasidharan, Anti Candida activity and brine shrimp toxicity assay of Ganoderma boninense. PubMed. 16 (2012) 43–48.

[4]. D. Cör, Z. Knez, M. Knez Hrnčič, Antitumour, Antimicrobial, Antioxidant and Antiacetylcholinesterase Effect of *Ganoderma Lucidum* Terpenoids and Polysaccharides: A Review. Molecules. 23 (2018) 649.

[5]. M. Wang, F. Yu, Research Progress on the Anticancer Activities and Mechanisms of Polysaccharides from Ganoderma. Frontiers in pharmacology. 13 (2022) 891171.

[6]. D. Cör Andrejč, Z. Knez, M. Knez Marevci, Antioxidant, antibacterial, antitumor, antifungal, antiviral, anti-inflammatory, and neuro-protective activity of *Ganoderma lucidum*: An overview. Frontiers in Pharmacology. (2022) 13.

[7]. Y. Wu, F. Han, S. Luan, R. Ai, P. Zhang, H. Li, L. Chen, Triterpenoids from *Ganoderma lucidum* and Their Potential Anti-inflammatory Effects. Journal of Agricultural and Food Chemistry. 67 (2019) 5147–5158.

[8]. N. Sato, Q. Zhang, C. Ma, M. Hattori, Anti-human Immunodeficiency Virus-1 Protease Activity of New Lanostane-Type Triterpenoids from *Ganoderma sinense*. Chemical and Pharmaceutical Bulletin. 57 (2009) 1076–1080.

[9]. S. Supramani, N. A. Rejab, Z. Ilham, W. A. A. Q. I. Wan-Mohtar, S. Ghosh, Basal stem rot of oil palm incited by Ganoderma species: A review. Eur J Plant Pathol 164 (2022) 1–20.

[10]. Q-Z. Li, C. Xiong, W. C. Wong, L-W. Zhou, Medium composition optimization and characterization of polysaccharides extracted from *Ganoderma boninense* along with antioxidant activity. International Journal of Biological Macromolecules. 260 (2024) 129528–129528.

[11]. L. Zakaria, Basal stem rot of oil palm: the pathogen, disease incidence, and control methods. Plant Disease. 107, (2022) 603–615.

[12]. U. Yogabaanu, J. F. Weber, P. Convey, M. Rizman-Idid, S. A. Alias, Antimicrobial properties and the influence of temperature on secondary metabolite production in cold environment soil fungi. Polar Science. 14 (2017) 60–67.

[13]. A. L. Santos, M. Uemi, M. Ionta, R. Horvath, E. S. Kawafune, M. G. Soares, M. M. P. Tangerina, L. S. de Medeiros, M. J. P. Ferreira, P. Sartorelli, Molecular network for accessing polyketide derivatives from Phomopsis sp., an endophytic fungus of *Casearia arborea* (Salicaceae). Phytochemistry Letters. 42 (2021) 1–7.

[14]. A. Shankar, K. K. Sharma, Fungal secondary metabolites in food and pharmaceuticals in the era of multi-omics. Applied Microbiology and Biotechnology. 106 (2022) 3465–3488.

[15]. A. Messaili, M. Wang, N. Bandeira, MolNetEnhancer: Enhanced molecular networks by integrating metabolome mining and annotation tools. Metabolites. 9 (2019) 144.

[16]. J. Dai, W. Wang, F. He, X. Yu, Z. Liu, Y. Wang, D. Zou, Discovery of anti-inflammatory molecules from *Dendrobium officinale* based on activity labelled molecular networking and its alleviation effect on ulcerative colitis. Food Research International. (2025) 115888.
[17]. A. M. Marques, L. De Carvalho Brito, S. C. Mendonça, B. A. Gomes, F. Da Cunha Camillo, G. W. De Souza E Silva, A. L. F. Sampaio, S. G. Leitão, M. R. Figueiredo, An Integrated Strategy of UHPLC-ESI-MS/MS Combined with Bioactivity-Based Molecular Networking for Identification of Antitumoral Withanolides from *Athenaea fasciculata* (Vell.) I.M.C. Rodrigues & Stehmann. Molecules. 29 (2024) 4357.
[18]. V. P. Chavda, J. Feehan, V. Apostolopoulos, Inflammation: The Cause of All Diseases. Cells. 13 (2024) 1906.
[19]. D. J. Newman, G. M. Cragg, Natural products as sources of new drugs over the nearly four decades from 01/1981 to 09/2019. Journal of Natural Products. 83 (2020) 770–803.
[20]. G. Sibi, S. Rabina, Inhibition of Pro-inflammatory mediators and cytokines by *Chlorella Vulgaris* extracts. Pharmacognosy Research. 8 (2015) 118.
[21]. R. Sabaragamuwa, C. O. Perera, Total Triterpenes, Polyphenols, Flavonoids, and Antioxidant Activity of Bioactive Phytochemicals of *Centella asiatica* by Different Extraction Techniques. Foods, 12 (2023) 3972.
[22]. Y. S. Chan, K. P. Chong, Antimicrobial Activity and Metabolite Analysis of *Ganoderma boninense* Fruiting Body. Journal of Pure and Applied Microbiology. 14 (2020) 1213–1226.
[23]. M. D. L. Berdolaga, Analysis of Glycerol in Nipa (Nypa Fruticans Wurmb.) Kernel Extract (Nke) Using High Performance Liquid Chromatography (HPLC). Proceedings of International Exchange and Innovation Conference on Engineering & Sciences (IEICES). 8 (2022) 317-322.
[24]. W. Senghoi, N. Konsue, S. Qin, W. K. Klangbud, Anti-inflammatory, antioxidant, and anti-apoptotic properties of *Thunbergia laurifolia* Lindl. aqueous leaf extract on LPS-stimulated RAW 264.7 macrophages. South African Journal of Botany. 174 (2024) 946–953.
[25]. A. Hambali, N. A. Jusril, N. F. M. Hashim, N. A. Manan, S. K. Adam, M. Z. Mehat, M. I. Adenan, J. Stanslas, H. A. Hamid, The Standardized Extract of *Centella asiatica* and Its Fractions Exert Antioxidative and Anti-Neuroinflammatory Effects on Microglial Cells and Regulate the Nrf2/HO-1 Signaling Pathway. Journal of Alzheimer S Disease. 99 (2024) S119–S138.
[26]. S. Singh, G. Kaur, V. Mangla, M. K. Gupta, Quinoline and quinolones: promising scaffolds for future antimycobacterial agents. J Enzyme Inhib Med Chem. 30 (2015) 492–504.
[27]. L. Vetcher, H. G. Menzella, T. Kudo, T. Motoyama, L. Katz, The Antifungal Polyketide Ambruticin Targets the HOG Pathway. Antimicrobial Agents and Chemotherapy. (2007) 3734–3736.
[28]. K. Sułkowska-Ziaja, M. Balik, A. Szczepkowski, M. Trepa, G. Zengin, K. Kała, B. Muszy´nska, A Review of Chemical Composition and Bioactivity Studies of the Most Promising Species of Ganoderma spp. Diversity. 15 (2023) 882.
[29]. B. S. Sanodiya, Gulab S. Thakur, Rakesh K. Baghel, G. B.K.S. Prasad and P. S. Bisen, Ganoderma lucidum: A Potent Pharmacological Macrofungus. Current Pharmaceutical Biotechnology. 10 (2009) 717 – 742.
[30]. G. Castellano, F. Torrens, Information Entropy-Based Classification of Triterpenoids and Steroids from Ganoderma. Phytochemistry. 116 (2015) 305-313.
[31]. Z. Chen, W. Qin, H. Lin, Y., Liu, Y. Tian, X. Zhao, T. Ding, Y. Wang, T. Mao, J. Li, Y. Shen, Inhibitory effect of polysaccharides extracted from Changbai Mountain *Ganoderma lucidum* on periodontal inflammation. Heliyon. 9 (2023) e13205.
[32]. PubChem website: https://pubchem.ncbi.nlm.nih.gov/ (assessed on 11th May 2025).
[33]. K. Srinivas, T. R. Reddy, V. Himabindu, G. M. Reddy, N. J. Mohan, Synthesis and Antibacterial Activity of Novel Quinoxaline-5-Carboxamide Derivatives. Journal of Applicable Chemistry. 3 (2014) 1432-1439.
[34]. S. Boontha, B. Buranrat, K. Saepang, P. Temkitthawon, T. Pitaksuteepong, Cytotoxic, Cell Apoptosis, Colony Formation and Anti-Migratory Activity of Three Herbal Plant Extracts in MCF-7 Breast Cancer Cells. Nat. Life Sci. Commun. 24 (2025) E2025004.
[35]. S. Phimsen, B. Cheirsilp, A. Nuylert, Effects of Different Proteases on Degree of Hydrolysis and Antioxidant Activity of Mung Bean Hydrolysates. Proceedings of International Exchange and Innovation Conference on Engineering & Sciences (IEICES). 10 (2024) 653-658.